Fornix subdivisions and spatial learning: a diffusion MRI study

Carl J. Hodgetts [a,b,1], Mark Postans [b,c,1], Angharad N. Williams [d], Kim S. Graham [e], Andrew D. Lawrence [b,e,*]

[a] Department of Psychology, Royal Holloway University of London, Egham, Surrey, TW20 0EX, UK
[b] Cardiff University Brain Research Imaging Centre (CUBRIC), School of Psychology, Cardiff University, Cardiff, CF24 4HQ, UK
[c] Communicable Disease Surveillance Centre (CDSC), Public Health Wales, Cardiff, CF10 4BZ, UK
[d] Department of Psychology, Chaucer, Nottingham Trent University, 50 Shakespeare Street, Nottingham, NG1 4FQ, UK
[e] Department of Psychology, University of Edinburgh, Edinburgh, EH8 9JZ, UK

ARTICLE INFO

ABSTRACT

The fornix is the major fibre pathway linking the hippocampal formation with distal brain sites. Human and animal lesion studies show that the connections comprising the fornix are vital for specific attributes of episodic and spatial memory. The fornix, however, interconnects the hippocampal formation with an array of subcortical and cortical sites and it is not known which specific connections support spatial-mnemonic function. To address this, utilizing a partly previously published dataset (Hodgetts et al., 2020), we applied a novel deterministic tractography protocol to diffusion-weighted magnetic resonance imaging (dMRI) data from a group of healthy young adult humans who separately completed a desktop-based virtual reality analogue of the Morris water maze task. The tractography protocol enabled the two main parts of the fornix, delineated previously in axonal tracing studies in rodents and primates, to be reconstructed in vivo, namely the pre-commissural fornix (connecting the hippocampus to medial prefrontal cortex and with basal forebrain) and the post-commissural fornix (linking the hippocampus and medial diencephalon). We found that inter-individual differences in pre-commissural – but not, surprisingly, post-commissural – fornix microstructure (indexed by free water corrected fractional anisotropy, FA) were significantly correlated with individual differences in spatial learning, indexed by reduction in search error as individuals learned to navigate to a hidden target location from multiple starting points. Specifically, higher FA in the pre-commissural fornix was associated with faster learning rates. This study provides novel evidence that flexible and/or precise spatial learning involves a hippocampal-basal forebrain/prefrontal network underpinned in part by the pre-commissural fornix.

1. Introduction

The fornix is the major white matter tract connecting the hippocampal formation with distal brain sites (Saunders and Aggleton, 2007). Decades of neuropsychological evidence reveals that the integrity of the fornix is critical for episodic memory in humans and flexible spatial memory in rodents and primates (Gaffan and Gaffan, 1991; Gaffan, 1992; McMackin et al., 1995; Aggleton and Brown, 1999; Aggleton et al., 2023).

While the fornix interconnects the hippocampal formation with numerous subcortical and cortical structures (Aggleton et al., 2010; Saunders and Aggleton, 2007), longstanding accounts of the neural substrates of episodic memory emphasise the importance of the direct hippocampal (HPC) projections to the anterior thalamic nuclei (ATN), along with the indirect fornical projections via the mammillary bodies (MB) to the ATN (Gaffan, 1992; Aggleton and Brown, 1999). According to Aggleton and Brown (1999) (see Aggleton et al., 2023 for subsequent developments) a common feature of anterograde amnesia is damage to any one of these structures, which collectively form an "extended hippocampal-diencephalic system" required for the encoding of new episodic information, binding the information to a spatial (and temporal) context, thus aiding subsequent recollection (Aggleton and Brown, 1999).

Direct tests of the functional unity of such a system have largely

---

come from tests of allocentric spatial memory in rodents, informed by cognitive map theory (O'Keefe and Nadel, 1978), which posits that a fundamental function of the hippocampus (HPC) is the construction and maintenance of allocentric spatial maps of the environment, providing a spatial (and temporal) context that 'scaffolds' episodic memories (O'Keefe and Nadel, 1979; for an alternative account, see Eichenbaum et al., 1999). Studies using tasks that tap allocentric spatial processing, such as T-maze place alternation, or the Morris water maze (MWM) (Morris et al., 1982), have revealed that normal performance depends on the integrity of the HPC, fornix, MB, and ATN (Aggleton and Brown, 1999; Aggleton and O'Mara, 2022), consistent with the notion that the individual structures forming an extended hippocampal-diencephalic system function conjointly to support flexible spatial memory.

Likewise, HPC, fornix, MB, and ATN lesions result in equivalent levels of impairment on an object-in-place scene discrimination learning task in monkeys (Gaffan,1994; Parker and Gaffan, 1997a, 1997b; Murray et al., 1998). This task requires monkeys to learn and remember the location of a discrete object in a unique spatial scene and incorporates elements of both spatial and episodic-like memory (Gaffan, 1994). Equivalent levels of impairment on this task are seen in humans with fornix damage (Aggleton et al., 2000).

Complementing these findings, studies using diffusion-weighted magnetic resonance imaging (dMRI) in humans have found associations between inter-individual differences in fornix microstructure and inter-individual differences in scene recollection (Rudebeck et al., 2009), the spatio-temporal detail of autobiographical memories (Hodgetts et al., 2017), scene discrimination learning (Postans et al., 2014), and scene perceptual discrimination (Hodgetts et al., 2015; Read et al., 2025).

Prior lesion and dMRI studies have typically treated the fornix as a unitary tract. However, it is a complex fibre pathway with two main parts. The fornix bifurcates at the anterior commissure into a post-commissural (pocfx) and a pre-commissural (precfx) fornix segment (Aggleton et al., 2010). Most fornix fibres pass caudal to the anterior commissure to form the pocfx. These fibres originate in the subicular complex and terminate into the medial MB and en route also convey fibres into the ATN (Aggleton et al., 2010; Christiansen et al., 2016b). Other fibres, which originate in both the HPC proper (i.e CA fields) and the subiculum (Saunders and Aggleton, 2007), pass rostral to the anterior commissure as the precfx. These fibres travel anteriorly to terminate in the septal nuclei, nucleus accumbens (NAcc), and mPFC (Poletti & Creswell,1977; Jay and Witter, 1991; Cenquizca and Swanson, 2007).

Although a few studies have attempted to compare the impact of selective pocfx versus precfx lesions on learning and memory (Macdougall and Capobianco, 1976; Henderson and Greene, 1977; Thomas, 1978; Tonkiss et al., 1990), it has proven challenging to confine damage to the target tract. An alternative approach is to use diffusion MRI tractography to isolate pocfx fibres (passing behind the anterior commissure) from precfx fibres (passing in front of the anterior commissure) (see Fig. 2, method) (Christiansen et al., 2016a). Using this approach, in a sample of healthy older adults, Christiansen et al. (2016a) found a correlation between pocfx, but not precfx, microstructure and inter-individual differences in visual recall from the Doors and People test (Baddeley et al., 1994). Similarly, Coad et al. (2020) found an association between pocfx, but not precfx microstructure and paired-associate object-in-location learning (PAL) (Lee et al., 2003). Together, these findings further support the importance of hippocampal-diencephalic connections in episodic and spatial memory.

Despite the emphasis on the direct fornical projections to the ATN, along with the indirect fornical projections via the MB, in current accounts of episodic and spatial memory, there are indications that other HPC connections conveyed via the fornix may play an important role in both episodic memory and spatial learning. In particular, regions of medial prefrontal cortex (mPFC), directly connected (ipsilaterally) with the HPC (subiculum/CA1) by the precfx in both rodents (Jay and Witter, 1991; Cenquizca and Swanson, 2007) and primates (Barbas and Blatt,

1995; Aggleton et al., 2015), may be important for aspects of flexible goal-directed episodic and spatial memory in both rodents (Euston et al., 2012; Eichenbaum et al., 2017) and humans (Preston and Eichenbaum, 2013; Murray et al., 2017; Patai and Spiers, 2021).

One line of evidence comes from the study of allocentric spatial learning in tasks including the MWM. As with HPC lesions (Morris et al., 1982), fornix-transected rodents are impaired in learning this task when they are required to navigate flexibly from multiple start positions, but not when learning to navigate along a single route (Eichenbaum et al., 1990; Compton et al., 1997). An identical pattern of impairment is seen following lesions of mPFC (Compton et al., 1997; see also Sutherland et al., 1982). Disconnecting the two structures by silencing the HPC of one hemisphere and the mPFC of the contralateral hemisphere ('crossed lesions') mimics this impairment (Wang and Cai, 2008; see also Churchwell et al., 2010), indicating that goal-directed memory tasks seem to require intact functions of both HPC and mPFC and their functional interactions (for additional findings and reviews see Eichenbaum et al., 2017; Poucet and Hok, 2017; Ito, 2018).

Further evidence for the importance of HPC-mPFC interactions in spatial navigation in humans comes from fMRI studies, which have shown increased HPC-mPFC functional coupling during the adoption of an allocentric spatial virtual reality (VR) navigation strategy (Dahmani and Bohbot, 2015) and between subiculum and mPFC during VR navigational planning (Brown et al., 2016), as well as reduced HPC-mPFC functional coupling in individuals with developmental topographical disorientation (Iaria et al., 2014), a selective orientation deficit characterised by an inability to form cognitive maps. More recently, using lesion network mapping, Roseman et al. (2024) found that bilateral HPC and mPFC are key nodes in a network defined by resting-state functional connectivity (RSFC), damage to which impairs topographical navigation.

While these functional interactions likely reflect, at least in part, the influence of HPC on mPFC, neither crossed lesion disconnections nor fc-MRI can determine a direction of effect when two target sites are reciprocally linked. Both HPC and mPFC receive and send projections to multiple cortical and subcortical areas, and so there are many pathways by which the hippocampus and mPFC could functionally interact, beyond the direct HPC-to-mPFC connections via the precfx. These routes include relays via parahippocampal cortices and via subcortical sites, including the nucleus reuniens and the anterior thalamic nuclei (Prasad and Chudasama, 2013; Anderson et al., 2016; Eichenbaum, 2017; Dolleman-van der Weel et al., 2019). It remains unclear then, whether the precfx plays an important role in flexible spatial learning.

In a prior publication (Hodgetts et al., 2020; see also Evensmoen et al., 2025), we provided initial evidence for the involvement of the human fornix in spatial learning, showing that microstructure of the fornix (reconstructed as a single tract) in healthy young adults was related to individual differences in learning to navigate to a hidden target location from multiple starting positions in a desktop-based VR analogue of the MWM task that is also sensitive to HPC lesions (Kolarik et al., 2018). Notably, the association between fornix microstructure and learning held when controlling for HPC volumes, which were not related to learning (for wider discussion see Weisberg and Ekstrom, 2021). Here, we present a novel analysis of this dataset, building on our prior publication in two ways. First, based on the protocol of Christiansen et al. (2016a) we used dMRI tractography to separately reconstruct the fibres forming the pocfx and those forming the precfx, and evaluated their microstructure based on the two-compartment free water elimination model, which enables more accurate estimation of tissue diffusion properties by mitigating the partial volume effects caused by free water (Pasternak et al., 2009).

Second, advancing our previous analysis of virtual navigation learning, which used latency to find the hidden target location as a performance metric, we adapted a proximity-to-goal measure of navigational efficiency previously used in studies of the MWM (Gallagher et al., 2015; see methods for details). Proximity – and related spatial

precision-based measures –are more sensitive to individual differences in MWM learning in rodents (Gallagher et al., 2015) and to the impact of HPC damage on desktop-based virtual navigation in humans (Kolarik et al., 2018). Finally, again consistent with studies of the MWM (Gallagher et al., 2015; Tomas Pereira and Burwell, 2015), we used a curve-fitting approach to compute a sensitive single graded index of spatial learning based on change in proximity-to-goal (i.e., reduction in search error) across learning trials, suitable for correlational analysis with fornix microstructure metrics. Using these more anatomically- and behaviourally-precise measures, we examined the relationship between microstructure of the pocfx and precfx and learning rate, providing novel insights into the fornical connections underpinning flexible and/or precise allocentric spatial learning in humans.

2. Method

2.1. Participants

Thirty-three healthy adult volunteers (15 men, 18 women; mean age = 24 years, range = 19–33 years) gave written informed consent to participate in this study. Portions of this data have been published previously (Hodgetts et al., 2020). Here we address a novel and distinct question, combining a new analytic approach to measure the precision of spatial learning, and a novel anatomically informed tractography protocol for reconstructing distinct fornix divisions. Participants were scanned at the Cardiff University Brain Research Imaging Centre (CUBRIC) and completed a VR analogue of the MWM in a separate cognitive testing session. All participants were fluent English speakers with normal or corrected-to-normal vision. The study was approved by the Cardiff University School of Psychology Research Ethics Committee.

2.2. Desktop VR navigation task

This article constitutes a novel analysis of data from a previously published study (Hodgetts et al., 2020), with detailed methods reported here in line with the recommendations of Thornberry et al. (2021).

Participants completed the virtual navigation task reported by Kolarik et al. (2018). The task was implemented using Unity 3D (Unity Technologies, San Francisco) and required participants to use the arrow keys on a keyboard to explore a 3D virtual art gallery from a first-person perspective (see Fig. 1 for task schematic).

The gallery room was 8 x 8 virtual metres, with 4 unique artworks, unevenly spaced, one on each wall, acting as landmarks. On a given trial, participants were required to locate a hidden sensor on the floor as quickly as possible. The hidden target was a 0.4 x.4 virtual metre square, occupying 0.25 % of the total room area, whose position was fixed across consecutive trials. When participants' search trajectory intersected the hidden sensor, it became visible and the caption "You found the hidden sensor" was shown in the centre of the screen.

Upon finding the sensor, a 10-s countdown appeared in the top left corner of the screen, which allowed participants to freely navigate and check their location with respect to the landmarks (the artworks) in the room before the next trial commenced. Following the countdown, an inter-trial screen appeared, and participants were able to click on a button to commence the next learning trial.

The maximum 'free-search' duration of each trial was 60 s. If a participant did not find the sensor within this timeframe, it became visible to allow the participant to move to and end the trial at the target location. Where this occurred, participants' position and cumulative proximity to the target (see below) continued to be tracked during this additional 'cued-navigation' period.

The task involved 20 learning trials, which were divided into five blocks of four trials. In each of these blocks, participants started the trial from one of four possible starting positions (arbitrary North, South, East, West). Participants began from the North on trials 1, 7, 10, 16 and 19; the South on trials 4, 6, 9, 13 and 18; the West on trials 3, 8, 11, 14, and
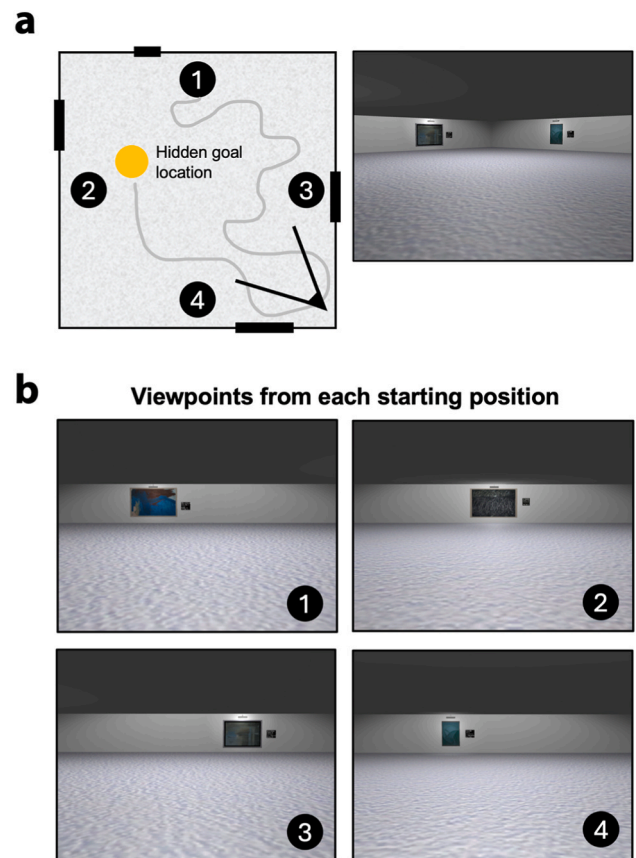
Fig. 1. The desktop VR navigation task. (A) Bird's-eye schematic and corresponding first-person view of the virtual art gallery arena that participants were required to navigate. Each wall of the arena features a painting that served as a 'landmark'. Points 1, 2, 3, and 4 correspond to the arbitrary North, West, East, and South starting positions, respectively. (B) First-person viewpoints from each of the four starting positions, showing the painting landmarks used in the task.

17; and the East on trials 2, 5, 12, 15 and 20.

Each participant's search trajectory was automatically recorded to a text file as Cartesian coordinates, at a frequency of 20 Hz.

2.3. MRI acquisition

Imaging data were acquired using a 3T GE Signa HDx MRI scanner (GE Healthcare) with an 8-channel receive-only head coil, at Cardiff University's Brain Research Imaging Centre (CUBRIC). A standard T1-weighted 3D FSPGR sequence (178 axial slices, 1 mm isotropic resolution, TR/TE = 7.8/3.0s, FOV = 256 × 256 × 176 mm, 256 × 256 x 176 data matrix, 20° flip angle) provided high-resolution anatomical images.

A diffusion weighted single-shot spin-echo Echo-Planar Imaging (EPI) pulse sequence was used to acquire whole-brain dMRI data (60 contiguous slices acquired along an oblique-axial plane with 2.4 mm thickness and no gap, TE = 87 ms; voxel dimensions = 2.4 × 2.4 × 2.4 mm^3; FOV = 23 × 23 cm^2; 96 × 96 acquisition matrix). The acquisition was cardiac gated, with 30 isotropic directions at b = 1200 s/mm^2. In addition, three non-diffusion weighted images were acquired with b = 0 s/mm^2.

2.4. Diffusion MRI preprocessing

DWI preprocessing, including correction for participant head motion and Eddy currents, was performed with ExploreDTI v 4.8.3 (Leemans et al., 2009). We used custom MATLAB scripts to perform
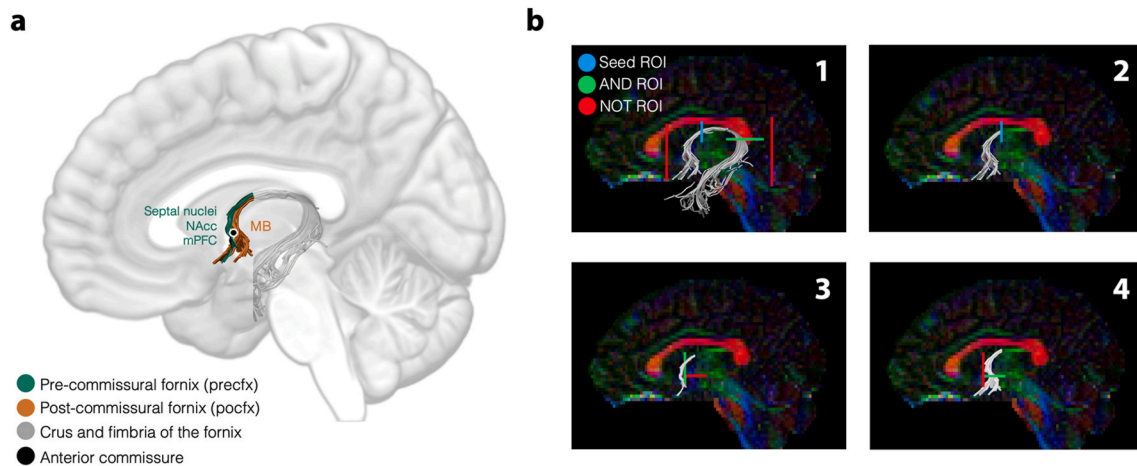
Fig. 2. Pre- and post-commissural fornix segmentation. (A) Schematic illustration of the anatomical landmarks used to differentiate pre- and post-commissural fornix segments (shown in green and orange, respectively). The key termination sites of the precfx and pocfx based on anatomical tract tracing studies are shown beside each tract segment in their respective colour (see main text; mPFC = medial prefrontal cortex; MB = mammillary bodies; NAcc = nucleus accumbens). (B) Approach and waypoint ROIs used for reconstructing the precfx and pocfx in ExploreDTI (see Sections 2.5.1 and 2.5.2 for further detail). (For interpretation of the references to colour in this figure legend, the reader is referred to the Web version of this article.)

free-water-elimination (FWE) based on a bi-tensor model to separate isotropic (free water) and anisotropic (tissue) diffusion compartments (Pasternak et al., 2009). This FWE pipeline includes spatial regularization (since estimation of the model is ill-posed in single shell dMRI) (Pasternak et al., 2009). FWE mitigates the adverse impact of CSF partial volume on diffusion tensor (DTI) metrics. This is especially crucial when examining the fornix, which borders the 3rd ventricle (De Santis et al., 2014).

Following FWE, corrected voxel-wise DTI indices were computed. Fractional Anisotropy (FA) – a dimensionless DTI-based index proposed to reflect axonal organization (Basser, 1997), represents the extent to which diffusion within biological tissue is anisotropic (restricted along a single axis) and can range from 0 (isotopic diffusion) to 1 (anisotropic diffusion). The resulting FA maps were inputs for tractography.

2.5. Tractography

Deterministic tractography was performed from all voxels based on constrained spherical deconvolution (CSD) (Jeurissen et al., 2011). CSD allows for the representation of bending/crossing/kissing fibres in individual voxels, as multiple peaks in the fibre orientation density function (fODF) can be extracted within each voxel (Dell'Acqua and Tournier, 2019). The step size was 1 mm, and the fODF amplitude threshold was 0.1. An angle threshold of 30° was used to prevent the reconstruction of anatomically implausible fibres.

To generate 3D fibre reconstructions of each tract segment, waypoint region-of-interest (ROI) gates were drawn manually onto whole-brain FWE-corrected FA maps. The waypoint ROIs defined the tracts based on a 'SEED' point and Boolean logical operations: 'NOT' and 'AND'. The 'NOT' and 'AND' gates corresponded to whether tracts passing through were omitted from analyses or retained, respectively. These gates were combined to reconstruct the tracts, based on anatomical plausibility (Schilling et al., 2020). Initially, a multiple ROI approach was applied to reconstruct the fornix and subsequently fornix tract division was performed.

2.5.1. Fornix reconstruction

The fornix was initially reconstructed in its entirety using a multiple-ROI approach (Hodgetts et al., 2017). A 'SEED' ROI encapsulating the fornix body was drawn on a coronal section. This was combined with an 'AND' ROI drawn on an axial section immediately inferior to the splenium of the corpus callosum, with an area sufficient to capture the crus

fornici. Exclusionary 'NOT' ROIs were drawn on an axial section covering the corpus callosum body, and on coronal sections covering the whole brain immediately anterior to the fornix pillars and posterior to the crus fornici. Post hoc exclusionary 'NOT' ROIs were drawn to exclude any extant spurious streamlines as required. The anterior body of the fornix was then split into its pocfx and precfx column segments (Fig. 2).

2.5.2. Pre- and post-commissural fornix segmentation

The anterior body of the fornix was first extracted from the fornix reconstructions using the 'splitter' tract segmentation tool within ExploreDTI (see Fig. 2), by drawing an 'AND' ROI immediately anterior to the existing 'SEED' ROI (see previous section), at the point where the tract descends towards the crus fornici. This step removed the crus and fimbria components from the fornix reconstructions, and was performed to minimise the risk of partial volume effects in the final segmentations due to an intermingling of pocfx and precfx streamlines as they progress into and beyond the crus fornici (Saunders and Aggleton, 2007).

The anterior body of the fornix was then further divided into its precfx and pocfx segments. The precfx was extracted by drawing an additional 'AND' ROI on a coronal section at the level of the AC, and an exclusionary 'NOT' ROI that intersected this 'AND' ROI on an axial section. To reconstruct the pocfx, the placement of these ROIs was swapped. Fibre streamlines were therefore only included in the precfx segmentations if they extended anterior to the AC, whereas the pocfx segmentations retained only those streamlines that descended posterior to the AC (see Fig. 2 for representative reconstructions).

Previous studies using the current protocol (Christiansen et al., 2016; Coad et al., 2020) have established that it can reliably distinguish the pre-commissural from the post-commissural fornix and that microstructure metrics extracted from the tracts can show high levels of inter-rater reliability. This reliability reflects, in part, the ease with which the key anatomical landmark for this tract segmentation approach (i.e., the anterior commissure) can be visually identified on colour-encoded FA maps.

2.6. Search trajectory and spatial learning analyses

In our earlier publication (Hodgetts et al., 2020), performance on each learning trial was defined by the time (in seconds) to reach the hidden target sensor. Latencies to find a target location are, however, a relative imprecise measure of place learning (Gallagher et al., 2015).

To increase sensitivity to inter-individual differences in spatial learning, for each learning trial, participants' proximity to the centre of the hidden sensor was sampled at 1-s intervals for the duration of their search, and this data was summed to compute a *cumulative proximity* measure (Gallagher et al., 2015). Participants whose search area is concentrated near the sensor will have a lower cumulative proximity score (i.e., smaller cumulative search error) compared to individuals that spend an equivalent time searching for the sensor but within a search area that is more widely distributed around the virtual room (see Supplementary Fig. S1). A lower score indicates that the subject's path is more direct and efficient toward the goal.

For each trial, participants' initial proximity to the sensor was subtracted from this cumulative proximity measure, since the 4 possible starting locations were non-equidistant from the target sensor. Prior research has demonstrated that proximity measures are more sensitive indices of allocentric place learning compared to latency metrics (Gallagher et al., 2015; Tomas Pereira and Burwell, 2015; Zhong et al., 2017).

As in our prior publication (Hodgetts et al., 2020), we then used a curve-fitting technique to derive a single participant-specific index of learning rate from these trial-wise cumulative proximity measures (for a similar approach in rodent studies of the MWM see Gallagher et al., 2015; Tomas Pereira and Burwell, 2015). Here, a learning curve was fit to subject-specific trial-wise cumulative proximity measures using a power function:

$$\text{Cumulative proximity} = a * x^b$$

The slope parameter (*b*) indicates the slope curvilinearity in individual subjects, with lower, more negative values, reflecting a more rapid descent from start to minimum search error (i.e., a faster learning rate).

As discussed in Hodgetts et al. (2020), simple curve-fitting techniques can, however, result in counterintuitive results when applied across all learning trials, such that some of the fastest learners will present the poorest model fits. For instance, this model provides a poor fit for individuals who learn the task quickly and plateau, but do not then sustain this level of performance until the learning trial series is completed (see example data from two participants in Fig. 3A; see
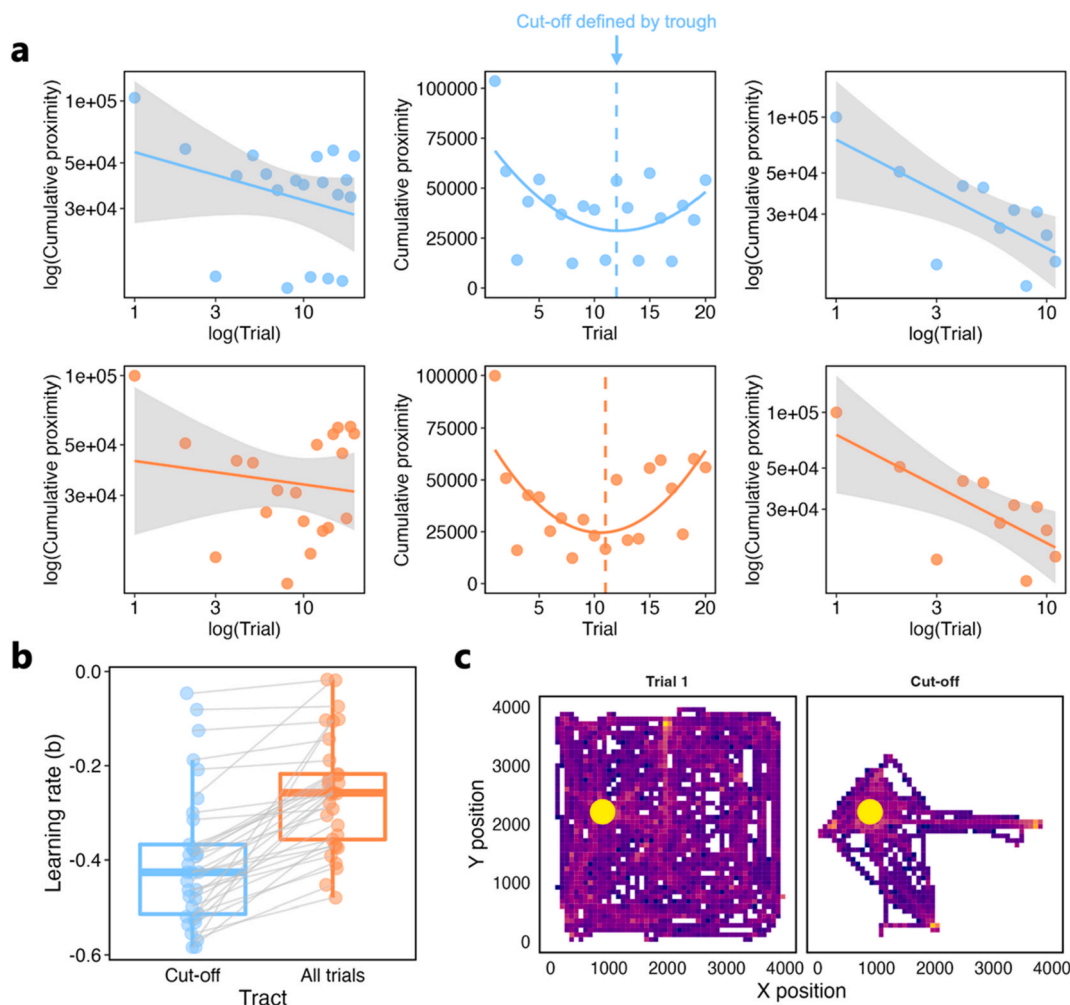

Fig. 3. The method used to determine the number of trials to-be-modelled in each participant. (A) Navigational learning data from two example participants are shown. Both display early learning followed by performance plateau and then poorer/more variable performance in later trials. A power function fits this pattern of cumulative proximity data poorly (left). To address this, a second-order polynomial was fitted to the trial-wise cumulative proximity data for each participant. The trial at which the first derivative of this polynomial crossed zero (i.e., the trough of the fitted curve) was taken as the point of minimum search error, and thus used to define the number of trials to be modelled (middle). Trials up to this participant-specific cut-off were then fit with a power function, and the *b* parameter was derived to index learning rate (right). Power fits were obtained by linearly fitting the log-transformed data. (B) Boxplot comparing values of the *b* parameter derived when using all trials (as in A, left) versus trials up to the cut-off (as in A, right). A statistical comparison of these fits can be found in the main text. (C) Group-level trajectory heatmaps illustrating participants' search paths relative to the hidden target (yellow circle) on Trial 1 and at the cut-off trial. On Trial 1, trajectories were widely dispersed across the arena; by the cut-off trial, search behaviour was more focused around the hidden sensor. Trajectories are collapsed across participants for visualisation purposes. (For interpretation of the references to colour in this figure legend, the reader is referred to the Web version of this article.)

Supplementary Fig. S2 for all learning curves). This pattern of performance may reflect cognitive/motivational factors (e.g., boredom induced mind-wandering or novelty seeking (Geana et al., 2016),) affecting performance in trials towards the end of the task (see also Gallagher et al., 2015; Tomas Pereira and Burwell, 2015 on the derivation of the so-called learning index measure used in rodent studies of the Morris Water Maze, in which later trials, by which time animals have already found the target location, are downweighted in the calculation of the learning index). To account for this complexity in learning patterns, we therefore used a data-driven approach to identify and apply a cut-off point to each individual participant's trial-wise performance data. A second-order polynomial model was fitted to everyone's trial-wise performance data using the Matlab curve-fitting toolbox (Mathworks, Inc.). The participant-specific cut-off was defined as the 'trough' of the resulting curve, at which point the first derivative of the second-degree polynomial crosses zero (Fig. 3, middle). All trials up to and including this participant-specific trial cut-off point were modelled using the power function described above (modal number of trials included = 13; range = 10–16). Critically, as shown in Fig. 3B, faster learning rates were observed for the truncated model compared to the model derived from all trials, and this difference was statistically significant (t(32) = −7.39, P < 0.001, d = −1.07). Further, the group location/trajectory heatmap for the participant-specific 'cut-off' trial illustrates that participants' searches converged around the target location and were not as randomly distributed around the arena compared to trial 1, consistent with successful place learning by the 'cut-off' trial (Fig. 3C).

2.7. Statistical analysis of fornix microstructure-learning rate associations

Frequentist statistical analyses were conducted in R (R Core Team, 2021).

Since higher FA is considered indicative of increased myelination, improved organisation, cohesion and compactness of white matter fibre tracts (Beaulieu, 2002) [indeed our previous studies have found that higher FA of the fornix "virtually dissected" as a single tract is associated with better spatial learning (Hodgetts et al., 2020); episodic memory (Hodgetts et al., 2017); and scene discrimination learning (Postans et al., 2014)], and lower (i.e. more negative) *b* values indicate faster learning (i.e. a more rapid decrease in cumulative search error across trials), we predicted a negative association between fornix FA and the learning rate parameter (*b*) (i.e. higher FA values would be associated with faster/more efficient learning). We therefore computed directional Pearson correlations between FA of the precfx and pocfx and learning rate, *b*. As we computed correlations across two tract segments, we applied a Bonferroni correction to our significance threshold, so that correlations with p < 0.025 were considered statistically significant.

Additional Bayesian correlation analyses were conducted using JASP (Version 0.19.3). From this, we report default Bayes factors and 95 % Bayesian credible intervals. The Bayes factor (BF) grades the intensity of the evidence that the data provide for the alternative hypothesis (H1) versus the null (H0) (or vice versa) on a continuous scale (Jeffreys, 1961; Wagenmakers et al., 2016).

Pearson correlations between learning rate and precfx and pocfx FA respectively were compared using a directional Steiger Z-test, computed using R package 'cocor', (Diedenhofen and Musch, 2015).

Prior to these analyses, following our earlier approach (Hodgetts et al., 2020; see also Guenzel et al., 2013) we identified and excluded participants whose cross-trial performance data did not provide robust evidence that place learning had occurred, for example, those not engaging with the task or those participants who randomly located the target very quickly on the first trial and who therefore had little opportunity to further improve performance across trials (i.e., 'non-learners'). This was achieved using a resampling approach in which an individual participant's cross-trial performance data was shuffled over 500 permutations to derive confidence intervals (CIs). Participants with

a model R^2 falling outside the 68 % CI (i.e., 1 SD) of their participant-specific random distribution were marked for exclusion from correlational analyses. Nine individuals were thus excluded (6 men, 3 women), and a two-tailed Welch's unequal variances *t*-test confirmed that the learning rates for these 'non-learners' (mean = −0.223, SD = 0.127) were significantly poorer than those derived from the retained participants (mean = −0.469, SD = 0.075; t (32) = −6.919, p < 0.001, d = −2.36). The nonlearners were not systematically different from the learners in age (mean age = 24 years in both groups). All subsequent analyses (including comparisons between tract segments) focused on those 'learner' participants (9 men, 15 women) whose trial-wise performance data provided robust evidence of successful place learning. [NB see Hodgetts et al. (2020) for a robustness check incorporating these participants, deriving an alternative non-slope-based measure of performance (mean latency to the cut-off) (which may index factors other than learning rate), finding a significant association between fornix microstructure and this index].

2.8. Data and code sharing

Anonymised output data and the code used within this project are freely available at https://osf.io/vsk3u/so that the figures and values reported in this manuscript are reproducible. However, ethical restrictions, relating to General Data Protection Regulation, do not allow for the public archiving of the raw study data. Access to pseudo-anonymised data could be granted after signing and approval of data transfer agreements. For this, readers should contact Dr Carl Hodgetts (carl.hodgetts@rhul.ac.uk) and Prof. Andrew Lawrence (andrew.d.lawrence@ed.ac.uk).

3. Results

3.1. Comparing fornix segment microstructure

We derived measures of participants' learning rates (*b* values; mean = −0.47, SD = 0.075) as well as FWE-corrected tract-averaged FA of the precfx (mean = 0.40, SD = 0.038) and pocfx (mean = 0.365, SD = 0.0446). FA of the precfx was significantly greater than that of the pocfx (t(23) = 3.223 p < 0.004, d = 0.831) (replicating the findings of Coad et al., 2020).

A two-tailed Pearson correlation revealed that precfx and pocfx FA measures were not significantly correlated (r(22) = 0.206, p = 0.335, BF_{01} = 2.545, 95 % [−0.204, 0.536] (Fig. 4).

Importantly, there was similar inter-individual variability in FA values across the two fornix segments (Pitman-Morgan test for (non) equality of variances (t (31) = 0.570, p = 0.573) (Fig. 4; computed using the 'PairedData' R package, Champely, 2018).

3.2. Correlation between fornix segment microstructure and spatial learning

For our planned analyses, we ran directional Pearson correlations between participants' learning rate (*b*) and fornix microstructure. These revealed a significant negative association between participant-specific learning rate parameter and precfx FA (r(22) = −0.443, p = 0.015, BF_{-0} = 4.591, 95 % CI [−0.079, −0.696], such that participants with higher precfx FA had faster learning rates [NB for the opposite association – i.e. lower precfx FA associated with faster learning rate, BF_{0+} = 11.50 in favour of the null]. By contrast, learning rate was not significantly correlated with pocfx FA (r(22) = 0.037, p = 0.569, BF_{0-} = 4.485, 95 % CI [−0.006, 0.411]) [NB for the opposite association – i.e. lower pocfx FA associated with faster learning rates, BF_{0+} = 3.44 in favour of the null]. Furthermore, the correlation between learning rate and precfx FA was significantly greater than that with pocfx FA (z = −1.884, p = 0.033; Fig. 5).
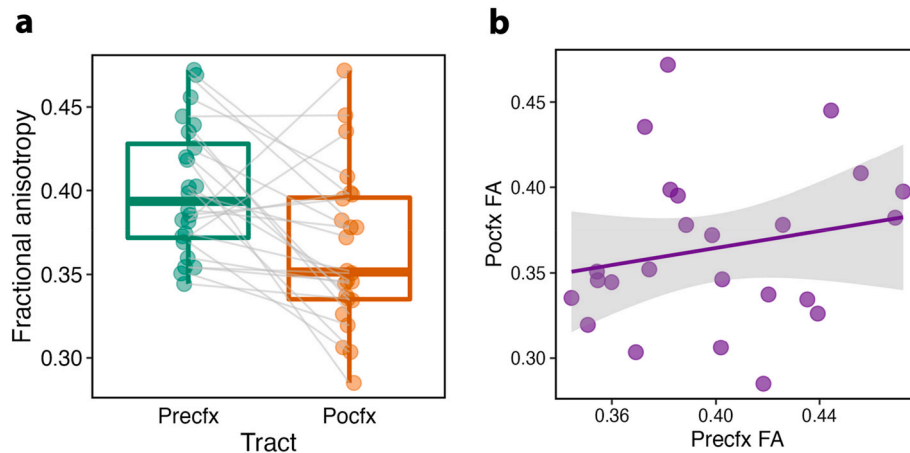
Fig. 4. Comparing fornix segment microstructure. (A) Boxplot comparing fractional anisotropy (FA) values for the precfx and pocfx, with individual data points shown. (B) Association between precfx and pocfx FA. The grey shaded area represents the 95 % confidence interval.
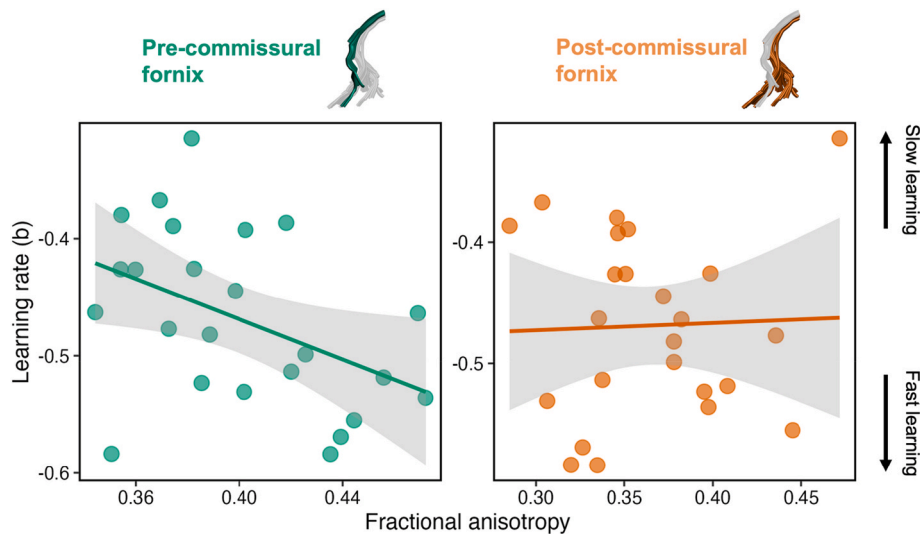

Fig. 5. The association between navigational learning rate (*b*) and precfx (left, green) versus descending pocfx FA (right, orange). The grey shaded area in each plot represents the 95 % CIs. (For interpretation of the references to colour in this figure legend, the reader is referred to the Web version of this article.)

3.3. Post hoc analysis: influence of sex on microstructure-learning correlations

Based on prior findings of sex differences in spatial navigation (including desktop VR MWM performance), typically characterised by a performance advantage for men, on average (Astur et al., 1998; Moffat et al., 1998; Woolley et al., 2010), we conducted a post hoc analysis to examine whether our main findings remained when controlling for sex (9 men, 15 women). The significant negative correlation between precfx FA and learning rate held when controlling for sex (r = −0.471, p = 0.024). Further, we observed no significant difference between men (mean = −0.494, SD = 0.081) and women (mean = −0.454, SD = 0.069) on our learning rate parameter (t(22) = 1.227, p = 0.215, d = 0.538).

4. Discussion

The fornix carries numerous projections both to, and from, the hippocampal formation, raising the fundamental question of which fornical pathways are most critical for spatial learning and memory (Aggleton et al., 2010). Here, we applied an anatomically guided diffusion tractography protocol to separately reconstruct pre-commissural (precfx)

and post-commissural (pocfx) fornix fibres in vivo (Christiansen et al., 2016a) and evaluate their microstructure, indexed by free water corrected fractional anisotropy (FA), in a healthy young adult sample. To capture inter-individual differences in spatial learning performance, we used a continuous, graded measure based on cross-trial improvement in proximity-to-target location in a desktop VR analogue of the MWM (Kolarik et al., 2018). This measure considers distance-to-the-goal along search trajectories and is more sensitive to relational, allocentric spatial strategy relative to search latencies alone (Gallagher et al., 2015). Using this approach, we found that inter-individual variation in precfx, but not pocfx, microstructure was significantly correlated with spatial learning, such that participants with higher FA in the precfx had faster learning rates, reflecting steeper (more rapid) cross-trial reductions in cumulative search error during learning. Our findings highlight, for the first time, the importance of one specific set of HPC connections for efficient flexible spatial learning in humans.

Anatomical tract tracing studies in rodents and primates show that the precfx principally innervates the septal nuclei (including medial and lateral septum), NAcc, and mPFC (Swanson and Cowan, 1977; Jay and Witter, 1991; Saunders and Aggleton, 2007; Aggleton et al., 2015). The precfx also provides a modest source of cholinergic input to the HPC from the medial septum -diagonal band complex (MSDB) (Mesulam

et al., 1983; MacLean et al., 1997). Precfx fibres do not, however, appear to innervate the diencephalon (Mathiasen et al., 2019). Since lesions of septal nuclei, NAcc and MSDB rarely result in impairments in allocentric spatial learning (Rawlins and Olton, 1982; Baxter et al., 1995; Floresco et al., 1996), our findings likely highlight the importance of connectivity between the HPC and mPFC mediated by the precfx in efficient and/or precise allocentric spatial learning.

While HPC place cells have long been established as the basis for a detailed representation of current location relative to the overall spatial layout, forming the elements of a cognitive map of space (O'Keefe and Nadel, 1978; Morris et al., 1982; Ekstrom et al., 2003; but see Eichenbaum et al., 1999 who argue that 'place' cells represent the set of experiences within a particular location), increasing evidence from rodent and human lesion and electrophysiological studies highlights a central role for the mPFC in goal representation, route planning, and top-down control of navigation (Ekstrom et al., 2003; Euston et al., 2012; Poucet and Hok, 2017; Patai and Spiers, 2021). Furthermore, both fMRI studies in humans (reviewed in Preston and Eichenbaum, 2013; Anderson et al., 2016; Patai and Spiers, 2021) and disconnection studies in rodents (reviewed in Eichenbaum, 2017; Murray et al., 2017) show that functional interactions between HPC and mPFC are critical for optimal performance on certain goal-directed memory tasks. In the domain of goal-directed spatial navigation, several recent models incorporate both HPC and mPFC into complex bidirectional circuitry in which map-based route planning requires finely coordinated interactions between 'bottom-up' spatial/contextual representations generated in the HPC and 'top-down' task/goal representations in the mPFC (Shapiro et al., 2014; Ito, 2018; Dolleman-van der Weel et al., 2019).

There are several pathways that could support HPC-mPFC functional interactions. One pathway for interaction involves a direct projection from the hippocampus to the PFC, and there are other indirect pathways through intermediary rhinal cortical and thalamic routes that are bidirectional (Prasad and Chudasama, 2013; Anderson et al., 2016; Aggleton and O'Mara, 2022; Messanvi et al., 2023). Critically in relation to our findings, the direct anatomical connectivity from HPC to mPFC is conveyed by the precfx. In rats, the entire longitudinal extent of the subiculum/CA1 is connected – via the precfx – with the mPFC, with connectivity increasing progressively in strength from dorsal to ventral hippocampus (Jay and Witter, 1991; Condé et al., 1995; Cenquizca and Swanson, 2007; Hoover and Vertes, 2007). Similarly in primates, the precfx provides the exclusive route for subiculum/CA1 projections to mPFC (Morecraft et al., 1992; Barbas and Blatt, 1995; Carmichael and Price, 1995; Aggleton et al., 1995), with relatively more projections arising from anterior HPC.

Recent findings challenge the traditional spatial-emotional dichotomy along the dorsal (posterior)-ventral (anterior) axis of the hippocampus (Moser and Moser, 1998), instead supporting a functional gradient (Strange et al., 2014), in line with the anatomical gradient described above. Lesion studies in rodents confirm that flexible spatial learning requires both the dorsal (dHPC) and intermediate/ventral (i/vHPC) hippocampus (Avigan et al., 2020; Hwang et al., 2024) (for related findings in humans see Kolarik et al., 2018). It has been suggested that vHPC plays a unique role in in interfacing between dHPC place-based and mPFC goal-based representations (McKenzie et al., 2016). Consistent with this, lesions of vHPC (Blanquat et al., 2013; Babl and Sigurdsson, 2025) and optogenetic silencing of monosynaptic vHPC-mPFC connections (Spellman et al., 2015) impair mPFC goal-location and goal-value encoding, while dHPC lesions and silencing do not.

In rodents, oscillatory synchrony is a key feature of bidirectional functional coupling between HPC and mPFC (Hyman et al., 2011; Eichenbaum, 2017; see also Chrastil et al., 2022 for related findings in humans using scalp-recorded EEG during VR maze-learning). The direction of the HPC-mPFC projection via the precfx aligns with the HPC-leading-mPFC directionality of information flow during spatial encoding-related increases in theta and gamma coherence between these regions seen during neural recordings in rodents (Siapas et al.,

2005; Spellman et al., 2015; Nardin et al., 2023; Lim et al., 2025), which depend upon the integrity of the ventral hippocampus (O'Neill et al., 2013). Since variation in the microstructural properties of white matter tracts can influence timing and synchronization of oscillatory activity between distal brain regions (Pajevic et al., 2014; Bells et al., 2017, 2019), individual differences in precfx microstructure may, therefore, impact the efficiency/fidelity of spatial information transfer from HPC to mPFC and hence the efficiency and/or precision of spatial learning.

Importantly, the precfx is not the only route by which spatial information can be transferred from HPC to mPFC. The nucleus reuniens (NRe) of the thalamus serves as a critical bidirectional relay between HPC and mPFC (Dolleman-van der Weel et al., 2019; Mathiasen et al., 2020; Messanvi et al., 2023; but see Andrianova et al., 2025) and has been argued to modulate HPC-mPFC theta coordination (Eichenbaum et al., 2017; Dolleman-van der Weel et al., 2019; but see de Mooij-van Malsen et al., 2023). Our findings are important therefore in clearly indicating that the direct HPC inputs to the PFC via the precfx are key to the functioning of broader bidirectional HPC-mPFC circuitry underpinning spatial learning and memory.

Notably, direct anatomical HPC-mPFC connectivity via the precfx is one-way. There are no direct return projections from mPFC to HC (Andrianova et al., 2023). Models of mPFC regulatory action upon the HPC emphasise the importance of indirect routes via the rhinal cortices as well as the nRe (Eichenbaum, 2017; Dolleman-van der Weel et al., 2019; Peng and Burwell, 2021; but see Andrianova et al., 2025). This circuitry is thought to enable executive control of HPC spatial representations to meet specific task demands. Experimental lesions and inactivation studies in rodents confirm the importance of this feedback: disrupting mPFC, lateral entorhinal cortex (ERC), or nRe function impairs task-dependent hippocampal activity and flexible navigation (Lu et al., 2013; Shapiro et al., 2014; Ito et al., 2015; Dolleman-van der Weel et al., 2019). Collectively, this bidirectional circuit, in which the precfx is a key link, helps to integrate the hippocampal cognitive map and a prefrontal abstract task 'map' or schema (Van de Maele et al., 2024). Spatial Information flows, at least in part via the precfx, 'bottom-up' from HPC during initial encoding of location and context, then 'top-down' from mPFC to bias future navigational trajectories based on goals and learned task rules. Coordination between these 'maps' is critical for prospective planning, decision-making, and optimising cognitive flexibility (Shapiro et al., 2014; Poucet and Hok, 2017; Ito, 2018; Samborska et al., 2022; Van de Maele et al., 2024).

Considering the emphasis placed on hippocampal-diencephalic connections mediated by the pocfx, but not the precfx, in longstanding accounts of episodic and spatial memory (Gaffan, 1992; Aggleton et al., 1999; Aggleton et al., 2023) it was somewhat surprising and significant that we found (using Bayes Factor hypothesis testing, Wagenmakers et al., 2016) substantial evidence *against* an association between pocfx microstructure and learning rate. One important caveat is that our pocfx tract reconstructions principally involve the connections of the HPC with the MB and largely exclude the projections to the ATN, since these turn immediately caudally to project into the ATN as the fornix columns descend to reach the MB (Poletti and Creswell, 1977; Christiansen et al., 2016b). The direct ATN projecting fibres do not form a discrete tract, but appear to remain diffuse (Mathiasen et al., 2019) and difficult to reconstruct with dMRI tractography (Özdemir et al., 2024). While lesion and crossed disconnection studies in rodents reveal the importance of these direct subicular-ATN connections for flexible spatial learning (Aggleton and O'Mara, 2022), including in the MWM (Warburton et al., 2000), nevertheless it is the case that complete fornix section can lead to greater impairments on certain tasks of spatial learning/memory (e.g., T-maze continuous alternation) than either ATN or MB lesions (Aggleton et al., 1995), further pointing to the importance of fornix connections beyond those linking the HPC with the diencephalon.

It might also be argued that a key difference between our findings and those in rodents and primates regarding the contribution of HPC-MB connections carried by the pocfx is that stationary desktop VR

navigation does not provide idiothetic, self-motion cues (see Starrett and Ekstrom, 2018 for discussion). Gaffan (1998) proposed that idiothetic cues generated by self-movement – whether of the whole body, limbs, or eyes – could, in theory, participate in object-in-place memory, and that the HPC and fornix provide such an idiothetic signal. However, lesion studies in rodents fail to support the idea that the fornix is important in conveying idiothetic information (Bussey et al., 2000).

Strikingly, and consistent with our findings, Vann and colleagues (Vann, 2013; Vann et al., 2011) have reported that selective lesions to the descending pocfx in rats, which completely disconnect the subicular projections to the MB, but spare those with the ATN, as well as sparing connections mediated by the precfx, have little-to-no impact on spatial memory tests, including the MWM and T-maze place alternation, that are sensitive to MB, mammillothalamic tract, ATN, and HPC lesions. A clear implication of these findings (with the caveat that they represent a single dissociation) is that the direct HPC-MB connectivity mediated by the pocfx may be less critical, and the direct HPC-mPFC connectivity mediated by the precfx more critical, to flexible spatial learning than previously highlighted in accounts of the extended hippocampal-diencephalic system (Gaffan, 1992; Aggleton and Brown, 1999). Notably, we (Williams et al., 2020) also found a correlation between individual differences in episodic autobiographical past and future thinking and precfx, but not pocfx, microstructure. Together, these findings highlight the potential importance of the direct HPC connections to mPFC carried by the precfx in the ability to flexibly form and utilise spatial/episodic representations in line with task demands (Eichenbaum, 2017; Murray et al., 2017).

Although our findings highlight the contributions of HPC connections conveyed by the precfx, this exercise is not exclusive, that is, demonstrating the importance of one set of connections does not negate the importance of other connections (Aggleton and O'Mara, 2022). Previous findings in humans link pocfx microstructure to other aspects of episodic memory (Christiansen et al., 2016a; Coad et al., 2020), including tests sensitive to MB pathology (Tsivilis et al., 2008), and there is clear evidence in rodents that subicular neurons targeting MB are critical for some forms of spatial memory (Li et al., 2025; Zhang et al., 2025). Understanding the complementary roles of the hippocampal-diencephalic and hippocampal-basal forebrain/prefrontal networks mediated by the fornix in learning and memory is an important future goal (Aggleton and O'Mara, 2022; McNaughton and Vann, 2022).

The present study has limitations that should be born in mind. Although FA is highly sensitive to the microstructure of fibers (De Santis et al., 2014), it lacks biological specificity, and may reflect myelination, axonal diameter, axonal density, and fibre dispersion (Beaulieu, 2002). Future multi-modal investigations using multi-shell diffusion MRI and advanced biophysical modelling to estimate specific tract microstructural properties, alongside measures of functional (oscillatory) connectivity using electrophysiological imaging with MEG (Karahan et al., 2022; Read et al., 2025) may provide further insight into the specific biological attributes and network interactions underlying the current microstructure-learning associations.

Furthermore, virtual tract renditions are created from estimations of water diffusion directionality, not from the anatomy itself, and characterization of fibres is limited by the MRI technology (e.g., higher gradient strengths enable dMRI acquisitions with higher spatial resolution, which enables the resolution of smaller white-matter bundles, Jones et al., 2018). Although we constructed virtual tract renditions using anatomical knowledge (Schilling et al., 2020), it is not possible to test the specificity of the tractography methods, for each participant, without knowing the true underlying anatomy (Grisot et al., 2021).

Whilst our sample size was comparable to related investigations (e. g., Brown et al., 2014; Chrastil et al., 2017), high statistical power provides greater precision in the estimation of the true effect size (Button et al., 2013). Critically, however, it is quite possible for low-power experiments to have high evidential value, and for high-power experiments to have low evidential value (Wagenmakers

et al., 2015). Here, default BFs >3 show that our findings provide substantial evidence, according to Jeffreys's (1961) conventions, for a positive correlation between precfx microstructure and learning, and, importantly, for a null correlation between pocfx microstructure and learning. That said, it will be important to extend our findings to larger samples, preferably using longitudinal and/or training designs that can examine the relationship between experience, brain microstructure, and spatial learning abilities (Sampaio-Baptista and Johansen-Berg, 2017; Coutrot et al., 2022).

In line with our hypothesis-driven analysis approach, based closely on the "gold standard" approach to analyzing allocentric spatial learning in the rodent Morris Water Maze (Gallagher et al., 2015), we utilised a spatial precision-based metric to assess learning. Further supporting the importance of this approach, a recent study found that individuals with fornix lesions showed intact schematic memory but impaired fine-grained detailed memory on sketch maps of recently and remotely experienced neighbourhoods and houses (Li et al., 2024). Nevertheless, we note that although our virtual maze task (VWM) and scoring protocol have strong validity (Gallagher et al., 2015; Kolarik et al., 2018), there are a plethora of VWM tasks and scoring protocols that are not standardised across research groups (see Thornberry et al., 2021 for discussion), making replication and generalization of experimental findings difficult. Future work in this area will benefit from adoption of better reporting standards, pre-registration of (standardised) protocols, scoring, and non-learner exclusion criteria, and reproducible analysis pipelines, similar to those suggested for studies of human threat learning (Lonsdorf et al., 2019).

In summary, we report a novel association between white matter microstructure of the precfx, but not pocfx, and inter-individual differences in flexible spatial learning. Together with similar findings in episodic memory (Williams et al., 2020), these findings help inform anatomical models of spatial and episodic memory and elucidate a potential anatomical substrate by which direct HPC-to-mPFC connectivity, as part of wider bidirectional HPC-mPFC circuitry, enable flexible encoding, retrieval, and recombination of spatial/episodic information in line with task demands (Eichenbaum, 2017; Murray et al., 2017).

CRediT authorship contribution statement

Carl J. Hodgetts: Writing – review & editing, Visualization, Validation, Funding acquisition, Formal analysis, Data curation, Conceptualization. **Mark Postans:** Writing – review & editing, Writing – original draft, Methodology, Formal analysis, Conceptualization. **Angharad N. Williams:** Writing – review & editing, Formal analysis. **Kim S. Graham:** Writing – review & editing, Supervision, Project administration, Funding acquisition. **Andrew D. Lawrence:** Writing – original draft, Supervision, Funding acquisition, Formal analysis, Conceptualization.

Declaration of competing interest

None.

Acknowledgements

Appendix A. Supplementary data

Supplementary data to this article can be found online at doi:

mmcdoino

Data availability

Anonymised output data and the code used within this project are freely available at https://osf.io/vsk3u/so that the figures and values reported in this manuscript are reproducible. However, ethical restrictions, relating to General Data Protection Regulation, do not allow for the public archiving of the raw study data. Access to pseudo-anonymised data could be granted after signing and approval of data transfer agreements. For this, readers should contact Dr Carl Hodgetts (carl.hodgetts@rhul.ac.uk) and Prof. Andrew Lawrence (andrew.d. lawrence@ed.ac.uk).

References

Aggleton, J.P., Brown, M.W., 1999. Episodic memory, amnesia, and the hippocampal–anterior thalamic axis. Behav. Brain Sci. 22 (3), 425–444. https://doi. org/10.1017/S0140525X99002034.

Aggleton, J.P., O'Mara, S.M., 2022. The anterior thalamic nuclei: core components of a tripartite episodic memory system. Nat. Rev. Neurosci. 23, 505–516. https://doi. org/10.1038/s41583-022-00591-8.

Aggleton, J.P., Neave, N., Nagle, S., Hunt, P.R., 1995. A comparison of the effects of anterior thalamic, mamillary body and fornix lesions on reinforced spatial alternation. Behav. Brain Res. 68 (1), 91–101. https://doi.org/10.1016/0166-4328 (94)00163-A.

Aggleton, J.P., McMackin, D., Carpenter, K., Hornak, J., Kapur, N., Halpin, S., et al., 2000. Differential cognitive effects of colloid cysts in the third ventricle that spare or compromise the fornix. Brain 123 (4), 800–815. https://doi.org/10.1093/brain/ 123.4.800.

Aggleton, J.P., O'Mara, S.M., Vann, S.D., Wright, N.F., Tsanov, M., Erichsen, J.T., 2010. Hippocampal–anterior thalamic pathways for memory: uncovering a network of direct and indirect actions. Eur. J. Neurosci. 31 (12), 2292–2307. https://doi.org/ 10.1111/j.1460-9568.2010.07251.x.

Aggleton, J.P., Vann, S.D., O'Mara, S.M., 2023. Converging diencephalic and hippocampal supports for episodic memory. Neuropsychologia 191, 108728. https://doi.org/10.1016/j.neuropsychologia.2023.108728.

Anderson, M.C., Bunce, J.G., Barbas, H., 2016. Prefrontal–hippocampal pathways underlying inhibitory control over memory. Neurobiol. Learn. Mem. 134, 145–161. https://doi.org/10.1016/j.nlm.2015.11.008.

Andrianova, L., Yanakieva, S., Margetts-Smith, G., Kohli, S., Brady, E.S., Aggleton, J.P., Craig, M.T., 2023. No evidence from complementary data sources of a direct glutamatergic projection from the mouse anterior cingulate area to the hippocampal formation. eLife 12, e77364. https://doi.org/10.7554/eLife.77364.

Andrianova, L., Banks, P.J., Booth, C.A., Brady, E.S., Margetts-Smith, G., Kohli, S., et al., 2025. Hippocampal pyramidal cells of the CA1 region are not a major target of the thalamic nucleus reuniens. PLoS Biol. 23 (10), e3003419. https://doi.org/10.1371/ journal.pbio.3003419.

Astur, R.S., Ortiz, M.L., Sutherland, R.J., 1998. A characterization of performance by men and women in a virtual morris water task: a large and reliable sex difference. Behav. Brain Res. 93 (1–2), 185–190. https://doi.org/10.1016/S0166-4328(98) 00019-9.

Avigan, P.D., Cammack, K., Shapiro, M.L., 2020. Flexible spatial learning requires both the dorsal and ventral hippocampus and their functional interactions with the prefrontal cortex. Hippocampus 30, 733–744. https://doi.org/10.1002/hipo.23198.

Babl, S.S., Sigurdsson, T., 2025. The dorsal and ventral hippocampus contribute differentially to spatial working memory and spatial coding in the prefrontal cortex. PLoS Biol. 23 (4), e3003140. https://doi.org/10.1371/journal.pbio.3003140.

Baddeley, A.D., Emslie, H., Nimmo-Smith, I., 1994. The Doors and People Test: a Test of Visual and Verbal Recall and Recognition. Bury St Edmunds: Thames Valley Test Company.

Basser, P.J., 1997. New histological and physiological stains derived from diffusion-tensor MR images. Ann. N. Y. Acad. Sci. 820, 123–138. https://doi.org/10.1111/ j.1749-6632.1997.tb46192.x.

Baxter, M.G., Bucci, D.J., Gorman, L.K., Wiley, R.G., Gallagher, M., 1995. Selective immunotoxic lesions of basal forebrain cholinergic cells: effects on learning and memory in rats. Behav. Neurosci. 109 (4), 714–722. https://doi.org/10.1037/0735-7044.109.4.714.

Beaulieu, C., 2002. The basis of anisotropic water diffusion in the nervous system–a technical review. NMR Biomed.: An International Journal Devoted to the Development and Application of Magnetic Resonance In Vivo 15 (7-8), 435–455. https://doi.org/10.1002/nbm.782.

Bells, S., Lefebvre, J., Prescott, S.A., Dockstader, C., Bouffet, E., Skocic, J., et al., 2017. Changes in white matter microstructure impact cognition by disrupting the ability of neural assemblies to synchronize. J. Neurosci. 37 (34), 8227–8238. https://doi.org/ 10.1523/JNEUROSCI.0560-17.2017.

Bells, S., Lefebvre, J., Longoni, G., Narayanan, S., Arnold, D.L., Yeh, E.A., Mabbott, D.J., 2019. White matter plasticity and maturation in human cognition. Glia 67 (11), 2020–2037. https://doi.org/10.1002/glia.23661.

Blanquat, P.D.S., Hok, V., Save, E., Poucet, B., Chaillan, F.A., 2013. Differential role of the dorsal hippocampus, ventro-intermediate hippocampus, and medial prefrontal

cortex in updating the value of a spatial goal. Hippocampus 23 (5), 342–351. https://doi.org/10.1002/hipo.22094.

Brown, T.I., Whiteman, A.S., Aselcioglu, I., Stern, C.E., 2014. Structural differences in hippocampal and prefrontal gray matter volume support flexible context-dependent navigation ability. J. Neurosci. 34 (6), 2314–2320. https://doi.org/10.1523/ JNEUROSCI.2202-13.2014.

Brown, T.I., Carr, V.A., LaRocque, K.F., Favila, S.E., Gordon, A.M., Bowles, B., et al., 2016. Prospective representation of navigational goals in the human hippocampus. Science 352 (6291), 1323–1326. https://doi.org/10.1126/science.aaf0784.

Bussey, T.J., Duck, J., Muir, J.L., Aggleton, J.P., 2000. Distinct patterns of behavioural impairments resulting from fornix transection or neurotoxic lesions of the perirhinal and postrhinal cortices in the rat. Behav. Brain Res. 111 (1–2), 187–202. https://doi. org/10.1016/S0166-4328(00)00155-8.

Button, K.S., Ioannidis, J.P., Mokrysz, C., Nosek, B.A., Flint, J., Robinson, E.S., Munafò, M.R., 2013. Confidence and precision increase with high statistical power. Nat. Rev. Neurosci. 14 (8), 585. https://doi.org/10.1038/nrn3475-c4, 585.

Carmichael, S.T., Price, J.L., 1995. Limbic connections of the orbital and medial prefrontal cortex in macaque monkeys. J. Comp. Neurol. 363 (4), 615–641. https:// doi.org/10.1002/cne.903630408.

Cenquizca, L.A., Swanson, L.W., 2007. Spatial organization of direct hippocampal field CA1 axonal projections to the rest of the cerebral cortex. Brain Res. Rev. 56 (1), 1–26. https://doi.org/10.1016/j.brainresrev.2007.05.002.

Champely, S., 2018. PairedData: paired data analysis. R package version 1.1.

Chrastil, E.R., Sherrill, K.R., Aselcioglu, I., Hasselmo, M.E., Stern, C.E., 2017. Individual differences in human path integration abilities correlate with gray matter volume in retrosplenial cortex, hippocampus, and medial prefrontal cortex. eNeuro 4 (2). https://doi.org/10.1523/ENEURO.0346-16.2017.

Chrastil, E.R., Rice, C., Goncalves, M., Moore, K.N., Wynn, S.C., Stern, C.E., Nyhus, E., 2022. Theta oscillations support active exploration in human spatial navigation. Neuroimage 262, 119581. https://doi.org/10.1016/j.neuroimage.2022.119581.

Christiansen, K., Aggleton, J.P., Parker, G.D., O'Sullivan, M.J., Vann, S.D., Metzler-Baddeley, C., 2016a. The status of the precommissural and postcommissural fornix in normal ageing and mild cognitive impairment: an MRI tractography study. Neuroimage 130, 35–47. https://doi.org/10.1016/j.neuroimage.2015.12.055.

Christiansen, K., Dillingham, C.M., Wright, N.F., Saunders, R.C., Vann, S.D., Aggleton, J. P., 2016b. Complementary subicular pathways to the anterior thalamic nuclei and mammillary bodies in the rat and macaque monkey brain. Eur. J. Neurosci. 43 (8), 1044–1061. https://doi.org/10.1111/ejn.13208.

Churchwell, J.C., Morris, A.M., Musso, N.D., Kesner, R.P., 2010. Prefrontal and hippocampal contributions to encoding and retrieval of spatial memory. Neurobiol. Learn. Mem. 93 (3), 415–421. https://doi.org/10.1016/j.nlm.2009.12.008.

Coad, B.M., Craig, E., Louch, R., Aggleton, J.P., Vann, S.D., Metzler-Baddeley, C., 2020. Precommissural and postcommissural fornix microstructure in healthy aging and cognition. Brain and neuroscience advances 4. https://doi.org/10.1177/ 2398212819899316, 2398212819899316.

Compton, D.M., Griffith, H.R., McDaniel, W.F., Foster, R.A., Davis, B.K., 1997. The flexible use of multiple cue relationships in spatial navigation: a comparison of water maze performance following hippocampal, medial septal, prefrontal cortex, or posterior parietal cortex lesions. Neurobiol. Learn. Mem. 68 (2), 117–132. https:// doi.org/10.1006/nlme.1997.3793.

Condé, F., Maire-lepoivre, E., Audinat, E., Crépel, F., 1995. Afferent connections of the medial frontal cortex of the rat. II. Cortical and subcortical afferents. J. Comp. Neurol. 352 (4), 567–593. https://doi.org/10.1002/cne.903520407.

Coutrot, A., Manley, E., Goodroe, S., Gahnstrom, C., Filomena, G., Yesiltepe, D., et al., 2022. Entropy of city street networks linked to future spatial navigation ability. Nature 604 (7904), 104–110. https://doi.org/10.1038/s41586-022-04486-7.

Dahmani, L., Bohbot, V.D., 2015. Dissociable contributions of the prefrontal cortex to hippocampus-and caudate nucleus-dependent virtual navigation strategies. Neurobiol. Learn. Mem. 117, 42–50. https://doi.org/10.1016/j.nlm.2014.07.002.

de Mooij-van Malsen, J.G., Röhrdanz, N., Buschhoff, A.S., Schiffelholz, T., Sigurdsson, T., Wulff, P., 2023. Task-specific oscillatory synchronization of prefrontal cortex, nucleus reuniens, and hippocampus during working memory. iScience 26 (9). https://doi.org/10.1016/j.isci.2023.107532.

De Santis, S., Drakesmith, M., Bells, S., Assaf, Y., Jones, D.K., 2014. Why diffusion tensor MRI does well only some of the time: variance and covariance of white matter tissue microstructure attributes in the living human brain. Neuroimage 89, 35–44. https:// doi.org/10.1016/j.neuroimage.2013.12.003.

Dell'Acqua, F., Tournier, J.D., 2019. Modelling white matter with spherical deconvolution: how and why? NMR Biomed. 32 (4), e3945. https://doi.org/ 10.1002/nbm.3945.

Diedenhofen, B., Musch, J., 2015. Cocor: a comprehensive solution for the statistical comparison of correlations. PLoS One 10 (4), e0121945. https://doi.org/10.1371/ journal.pone.0121945.

Dolleman-van der Weel, M.J., Griffin, A.L., Ito, H.T., Shapiro, M.L., Witter, M.P., Vertes, R.P., Allen, T.A., 2019. The nucleus reuniens of the thalamus sits at the nexus of a hippocampus and medial prefrontal cortex circuit enabling memory and behavior. Learn. Mem. 26 (7), 191–205. https://doi.org/10.1101/lm.048389.118.

Eichenbaum, H., 2017. Prefrontal–hippocampal interactions in episodic memory. Nat. Rev. Neurosci. 18, 547–558. https://doi.org/10.1038/nrn.2017.74.

Eichenbaum, H., Stewart, C., Morris, R.G., 1990. Hippocampal representation in place learning. J. Neurosci. 10 (11), 3531–3542. https://doi.org/10.1523/JNEUROSCI.10-11-03531.1990.

Eichenbaum, H., Dudchenko, P., Wood, E., Shapiro, M., Tanila, H., 1999. The hippocampus, memory, and place cells: is it spatial memory or a memory space? Neuron 23 (2), 209–226. https://doi.org/10.1016/S0896-6273(00)80773-4.

Ekstrom, A.D., Kahana, M.J., Caplan, J.B., Fields, T.A., Isham, E.A., Newman, E.L., Fried, I., 2003. Cellular networks underlying human spatial navigation. Nature 425 (6954), 184–188. https://doi.org/10.1038/nature01964.

Euston, D.R., Gruber, A.J., McNaughton, B.L., 2012. The role of medial prefrontal cortex in memory and decision making. Neuron 76 (6), 1057–1070. https://doi.org/10.1016/j.neuron.2012.12.002.

Evensmoen, H.R., Rimol, L.M., Håberg, A., 2025. Inferior and middle longitudinal fasciculus and fornix support allocentric representation. Hippocampus 35 (5), e70031. https://doi.org/10.1002/hipo.70031.

Floresco, S.B., Seamans, J.K., Phillips, A.G., 1996. Differential effects of lidocaine infusions into the ventral CA1/subiculum or the nucleus accumbens on the acquisition and retention of spatial information. Behav. Brain Res. 81 (1–2), 163–171. https://doi.org/10.1016/S0166-4328(96)00058-7.

Gaffan, D., 1992. The role of the hippocampus-fornix-mammillary system in episodic memory. In: Squire, L.R., Butters, N. (Eds.), Neuropsychology of Memory, second ed. The Guilford Press, pp. 336–346.

Gaffan, D., 1994. Scene-specific memory for objects: a model of episodic memory impairment in monkeys with fornix transection. J. Cognit. Neurosci. 6 (4), 305–320. https://doi.org/10.1162/jocn.1994.6.4.305.

Gaffan, D., 1998. Idiothetic input into object-place configuration as the contribution to memory of the monkey and human hippocampus: a review. Exp. Brain Res. 123, 201–209. https://doi.org/10.1007/s002210050562.

Gaffan, D., Gaffan, E.A., 1991. Amnesia in man following transection of the fornix: a review. Brain 114 (6), 2611–2618. https://doi.org/10.1093/brain/114.6.2611.

Gallagher, M., Burwell, R., Burchinal, M., 2015. Severity of spatial learning impairment in aging: development of a learning index for performance in the morris water maze. Behav. Neurosci. 129 (4), 540–548. https://doi.org/10.1037/bne0000080.

Geana, A., Wilson, R.C., Daw, N., Cohen, J.D., 2016. Boredom, information-seeking and exploration. Proceedings of the Annual Meeting of the Cognitive Science Society 38. Retrieved from. https://escholarship.org/uc/item/4rg9267w.

Grisot, G., Haber, S.N., Yendiki, A., 2021. Diffusion MRI and anatomic tracing in the same brain reveal common failure modes of tractography. Neuroimage 239, 118300. https://doi.org/10.1016/j.neuroimage.2021.118300.

Guenzel, F.M., Wolf, O.T., Schwabe, L., 2013. Stress disrupts response memory retrieval. Psychoneuroendocrinology 38 (8), 1460–1465. https://doi.org/10.1016/j.psyneuen.2012.12.010.

Henderson, J., Greene, E., 1977. Behavioral effects of lesions of precommissural and postcommissural fornix. Brain Res. Bull. 2 (2), 123–129. https://doi.org/10.1016/0361-9230(77)90008-9.

Hodgetts, C.J., Postans, M., Shine, J.P., Jones, D.K., Lawrence, A.D., Graham, K.S., 2015. Dissociable roles of the inferior longitudinal fasciculus and fornix in face and place perception. eLife 4, e07902. https://doi.org/10.7554/eLife.07902.

Hodgetts, C.J., Postans, M., Warne, N., Varnava, A., Lawrence, A.D., Graham, K.S., 2017. Distinct contributions of the fornix and inferior longitudinal fasciculus to episodic and semantic autobiographical memory. Cortex 94, 1–14. https://doi.org/10.1016/j.cortex.2017.05.010.

Hodgetts, C.J., Stefani, M., Williams, A.N., Kolarik, B.S., Yonelinas, A.P., Ekstrom, A.D., et al., 2020. The role of the fornix in human navigational learning. Cortex 124, 97–110. https://doi.org/10.1016/j.cortex.2019.10.017.

Hoover, W.B., Vertes, R.P., 2007. Anatomical analysis of afferent projections to the medial prefrontal cortex in the rat. Brain Struct. Funct. 212, 149–179. https://doi.org/10.1007/s00429-007-0150-4.

Hwang, H., Jin, S.W., Lee, I., 2024. Differential functions of the dorsal and intermediate regions of the hippocampus for optimal goal-directed navigation in VR space. eLife 13. https://doi.org/10.7554/eLife.97114.3. RP97114.

Hyman, J.M., Hasselmo, M.E., Seamans, J.K., 2011. What is the functional relevance of prefrontal cortex entrainment to hippocampal theta rhythms? Front. Neurosci. 5, 24. https://doi.org/10.3389/fnins.2011.00024.

Iaria, G., Arnold, A.E., Burles, F., Liu, I., Slone, E., Barclay, S., et al., 2014. Developmental topographical disorientation and decreased hippocampal functional connectivity. Hippocampus 24 (11), 1364–1374. https://doi.org/10.1002/hipo.22317.

Ito, H.T., 2018. Prefrontal–hippocampal interactions for spatial navigation. Neurosci. Res. 129, 2–7. https://doi.org/10.1016/j.neures.2017.04.016.

Ito, H.T., Zhang, S.J., Witter, M.P., Moser, E.I., Moser, M.B., 2015. A prefrontal–thalamo–hippocampal circuit for goal-directed spatial navigation. Nature 522 (7554), 50–55. https://doi.org/10.1038/nature14396.

Jeffreys, H., 1961. The Theory of Probability, third ed. Oxford University Press, Oxford, England.

Jeurissen, B., Leemans, A., Jones, D.K., Tournier, J.D., Sijbers, J., 2011. Probabilistic fiber tracking using the residual bootstrap with constrained spherical deconvolution. Hum. Brain Mapp. 32 (3), 461–479. https://doi.org/10.1002/hbm.22099.

Jones, D.K., Alexander, D.C., Bowtell, R., Cercignani, M., Dell'Acqua, F., McHugh, D.J., et al., 2018. Microstructural imaging of the human brain with a 'super-scanner': 10 key advantages of ultra-strong gradients for diffusion MRI. Neuroimage 182, 8–38. https://doi.org/10.1016/j.neuroimage.2018.05.047.

Karahan, E., Tait, L., Si, R., Özkan, A., Szul, M.J., Graham, K.S., et al., 2022. The interindividual variability of multimodal brain connectivity maintains spatial heterogeneity and relates to tissue microstructure. Commun. Biol. 5 (1), 1007. https://doi.org/10.1038/s42003-022-03974-w.

Kolarik, B.S., Baer, T., Shahlaie, K., Yonelinas, A.P., Ekstrom, A.D., 2018. Close but no cigar: spatial precision deficits following medial temporal lobe lesions provide novel insight into theoretical models of navigation and memory. Hippocampus 28 (1), 31–41. https://doi.org/10.1002/hipo.22801.

Lee, A.C., Rahman, S., Hodges, J.R., Sahakian, B.J., Graham, K.S., 2003. Associative and recognition memory for novel objects in dementia: implications for diagnosis. Eur. J. Neurosci. 18 (6), 1660–1670. https://doi.org/10.1046/j.1460-9568.2003.02883.x.

Leemans, A., Jeurissen, B., Sijbers, J., Jones, D.K., 2009. ExploreDTI: a graphical toolbox for processing, analyzing, and visualizing diffusion MR data. Proc Intl Soc Mag Reson Med 17 (1), 3537.

Li, A., Lei, X., Herdman, K., Waidergoren, S., Gilboa, A., Rosenbaum, R.S., 2024. Impoverished details with preserved gist in remote and recent spatial memory following hippocampal and fornix lesions. Neuropsychologia 194, 108787. https://doi.org/10.1016/j.neuropsychologia.2024.108787.

Li, L., Guo, Y., Jing, W., Tang, X., Zeng, J., Hou, Z., et al., 2025. Cell-type specific circuits in the mammillary body for place and object recognition memory. Adv. Sci., 2409397 https://doi.org/10.1002/advs.202409397.

Lim, H.Y., Park, S., Lee, I., 2025. Sequential development of task representation from hippocampus to prefrontal cortex supports goal-directed spatial navigation. bioRxiv. https://doi.org/10.1101/2025.10.05.680599.

Lonsdorf, T.B., Klingelhöfer-Jens, M., Andreatta, M., Beckers, T., Chalkia, A., Gerlicher, A., et al., 2019. Navigating the garden of forking paths: data exclusions in fear conditioning research. eLife 8, e52465. https://doi.org/10.7554/eLife.52465.

Lu, L., Leutgeb, J.K., Tsao, A., Henriksen, E.J., Leutgeb, S., Barnes, C.A., et al., 2013. Impaired hippocampal rate coding after lesions of the lateral entorhinal cortex. Nat. Neurosci. 16 (8), 1085–1093. https://doi.org/10.1038/nn.3462.

Macdougall, J.M., Capobianco, S., 1976. Dissociation of behavioral inhibition within the fornix system. Physiol. Behav. 17 (5), 755–760. https://doi.org/10.1016/0031-9384(76)90035-4.

Maclean, C.J., Baker, H.F., Fine, A., Ridley, R.M., 1997. The distribution of p75 neurotrophin receptor-immunoreactive cells in the forebrain of the common marmoset (Callithrix jacchus). Brain Res. Bull. 43 (2), 197–208. https://doi.org/10.1016/S0361-9230(96)00441-8.

Mathiasen, M.L., Louch, R.C., Nelson, A.D., Dillingham, C.M., Aggleton, J.P., 2019. Trajectory of hippocampal fibres to the contralateral anterior thalamus and mammillary bodies in rats, mice, and macaque monkeys. Brain and Neuroscience Advances 3, 2398212819871205. https://doi.org/10.1177/2398212819871205.

Mathiasen, M.L., O'Mara, S.M., Aggleton, J.P., 2020. The anterior thalamic nuclei and nucleus reuniens: so similar but so different. Neurosci. Biobehav. Rev. 119, 268–280. https://doi.org/10.1016/j.neubiorev.2020.10.006.

McKenzie, S., Keene, C.S., Farovik, A., Bladon, J., Place, R., Komorowski, R., Eichenbaum, H., 2016. Representation of memories in the cortical–hippocampal system: results from the application of population similarity analyses. Neurobiol. Learn. Mem. 134, 178–191. https://doi.org/10.1016/j.nlm.2015.12.008.

McMackin, D., Cockburn, J., Anslow, P., Gaffan, D., 1995. Correlation of fornix damage with memory impairment in six cases of colloid cyst removal. Acta Neurochir. 135 (1), 12–18. https://doi.org/10.1007/BF02307408.

McNaughton, N., Vann, S.D., 2022. Construction of complex memories via parallel distributed cortical–subcortical iterative integration. Trends Neurosci. 45 (7), 550–562. https://doi.org/10.1016/j.tins.2022.04.006.

Messanvi, K.F., Berkun, K., Perkins, A., Chudasama, Y., 2023. Parallel pathways provide hippocampal spatial information to prefrontal cortex. J. Neurosci. 43 (1), 68–81. https://doi.org/10.1523/JNEUROSCI.0846-22.2022.

Mesulam, M.M., Mufson, E.J., Levey, A.I., Wainer, B.H., 1983. Cholinergic innervation of cortex by the basal forebrain: cytochemistry and cortical connections of the septal area, diagonal band nuclei, nucleus basalis (substantia innominata), and hypothalamus in the rhesus monkey. J. Comp. Neurol. 214 (2), 170–197. https://doi.org/10.1002/cne.902140206.

Moffat, S.D., Hampson, E., Hatzipantelis, M., 1998. Navigation in a "virtual" maze: sex differences and correlation with psychometric measures of spatial ability in humans. Evol. Hum. Behav. 19 (2), 73–87. https://doi.org/10.1016/S1090-5138(97)00104-9.

Morecraft, R.J., Geula, C., Mesulam, M.M., 1992. Cytoarchitecture and neural afferents of orbitofrontal cortex in the brain of the monkey. J. Comp. Neurol. 323 (3), 341–358. https://doi.org/10.1002/cne.903230304.

Morris, R.G.M., Garrud, P., Rawlins, J.N., O'Keefe, J., 1982. Place navigation impaired in rats with hippocampal lesions. Nature 297 (5868), 681–683. https://doi.org/10.1038/297681a0.

Moser, M.B., Moser, E.I., 1998. Functional differentiation in the hippocampus. Hippocampus 8 (6), 608–619. https://doi.org/10.1002/(SICI)1098-1063(1998)8:6<608::AID-HIPO3>3.0.CO;2-7.

Murray, E.A., Baxter, M.G., Gaffan, D., 1998. Monkeys with rhinal cortex damage or neurotoxic hippocampal lesions are impaired on spatial scene learning and object reversals. Behav. Neurosci. 112 (6), 1291–1303. https://doi.org/10.1037/0735-7044.112.6.1291.

Murray, E.A., Wise, S.P., Graham, K.S., 2017. The Evolution of Memory Systems: Ancestors, Anatomy, and Adaptations. Oxford University Press, Oxford, UK.

Nardin, M., Kaefer, K., Stella, F., Csicsvari, J., 2023. Theta oscillations as a substrate for medial prefrontal-hippocampal assembly interactions. Cell Rep. 42 (9), 113015. https://doi.org/10.1016/j.celrep.2023.113015.

O'Keefe, J., Nadel, L., 1978. The Hippocampus as a Cognitive Map. Oxford University Press, Oxford, UK.

O'Neill, P.-K., Gordon, J.A., Sigurdsson, T., 2013. Theta oscillations in the medial prefrontal cortex are modulated by spatial working memory and synchronize with the hippocampus through its ventral subregion. J. Neurosci. 33 (35), 14211–14224. https://doi.org/10.1523/JNEUROSCI.2378-13.2013.

Özdemir, R., Lehtimäki, K., Siitama, E., Möttönen, T., Haapasalo, J., Järvenpää, S., et al., 2024. High angular resolution diffusion-weighted imaging and higher order tractography of the white matter tracts in the anterior thalamic area: insights into

deep brain stimulation targeting. Neuroimage: Report 4 (3), 100210. https://doi.org/10.1016/j.ynirp.2024.100210.

O'Keefe, J., Nadel, L., 1979. The cognitive map as a hippocampus. Behav. Brain Sci. 2 (4), 520–533. https://doi.org/10.1017/S0140525X00064256.

Pajevic, S., Basser, P.J., Fields, R.D., 2014. Role of myelin plasticity in oscillations and synchrony of neuronal activity. Neuroscience 276, 135–147. https://doi.org/10.1016/j.neuroscience.2013.11.007.

Parker, A., Gaffan, D., 1997a. Mamillary body lesions in monkeys impair object-in-place memory: functional unity of the fornix-mamillary system. J. Cognit. Neurosci. 9 (4), 512–521. https://doi.org/10.1162/jocn.1997.9.4.512.

Parker, A., Gaffan, D., 1997b. The effect of anterior thalamic and cingulate cortex lesions on object-in-place memory in monkeys. Neuropsychologia 35 (8), 1093–1102. https://doi.org/10.1016/S0028-3932(97)00042-0.

Pasternak, O., Sochen, N., Gur, Y., Intrator, N., Assaf, Y., 2009. Free water elimination and mapping from diffusion MRI. Magn. Reson. Med. 62 (3), 717–730. https://doi.org/10.1002/mrm.22055.

Patai, E.Z., Spiers, H.J., 2021. The versatile wayfinder: prefrontal contributions to spatial navigation. Trends Cognit. Sci. 25 (6), 520–533. https://doi.org/10.1016/j.tics.2021.02.010.

Peng, X., Burwell, R.D., 2021. Beyond the hippocampus: the role of parahippocampal-prefrontal communication in context-modulated behavior. Neurobiol. Learn. Mem. 185, 107520. https://doi.org/10.1016/j.nlm.2021.107520.

Poletti, C.E., Creswell, G., 1977. Fornix system efferent projections in the squirrel monkey: an experimental degeneration study. J. Comp. Neurol. 175 (1), 101–127. https://doi.org/10.1002/cne.901750107.

Postans, M., Hodgetts, C.J., Mundy, M.E., Jones, D.K., Lawrence, A.D., Graham, K.S., 2014. Interindividual variation in fornix microstructure and macrostructure is related to visual discrimination accuracy for scenes but not faces. J. Neurosci. 34 (36), 12121–12126. https://doi.org/10.1523/JNEUROSCI.0026-14.2014.

Poucet, B., Hok, V., 2017. Remembering goal locations. Curr. Opin. Behav. Sci. 17, 51–56. https://doi.org/10.1016/j.cobeha.2017.06.003.

Prasad, J.A., Chudasama, Y., 2013. Viral tracing identifies parallel disynaptic pathways to the hippocampus. J. Neurosci. 33 (19), 8494–8503. https://doi.org/10.1523/JNEUROSCI.5072-12.2013.

Preston, A.R., Eichenbaum, H., 2013. Interplay of hippocampus and prefrontal cortex in memory. Curr. Biol. 23 (17), R764–R773. https://doi.org/10.1016/j.cub.2013.05.041.

R Core Team, 2021. R: a Language and Environment for Statistical Computing. R Foundation for Statistical Computing, Vienna, Austria. https://www.R-project.org/.

Rawlins, J.N.P., Olton, D.S., 1982. The septo-hippocampal system and cognitive mapping. Behav. Brain Res. 5 (4), 331–358. https://doi.org/10.1016/0166-4328(82)90039-0.

Read, M.-L., Hodgetts, C.J., Lawrence, A.D., Evans, C.J., Singh, K.D., Umla-Runge, K., Graham, K.S., 2025. Multimodal MEG and microstructure-MRI investigations of the human hippocampal scene network. J. Neurosci. 45 (22), e1700242025. https://doi.org/10.1523/JNEUROSCI.1700-24.2025.

Roseman, M., Elias, U., Kletenik, I., Ferguson, M.A., Fox, M.D., Horowitz, Z., et al., 2024. A neural circuit for spatial orientation derived from brain lesions. Cerebr. Cortex 34 (1). https://doi.org/10.1093/cercor/bhad486 bhad486.

Rudebeck, S.R., Scholz, J., Millington, R., Rohenkohl, G., Johansen-Berg, H., Lee, A.C., 2009. Fornix microstructure correlates with recollection but not familiarity memory. J. Neurosci. 29 (47), 14987–14992. https://doi.org/10.1523/JNEUROSCI.4707-09.2009.

Samborska, V., Butler, J.L., Walton, M.E., Behrens, T.E., Akam, T., 2022. Complementary task representations in hippocampus and prefrontal cortex for generalizing the structure of problems. Nat. Neurosci. 25 (10), 1314–1326. https://doi.org/10.1038/s41593-022-01149-8.

Sampaio-Baptista, C., Johansen-Berg, H., 2017. White matter plasticity in the adult brain. Neuron 96 (6), 1239–1251. https://doi.org/10.1016/j.neuron.2017.11.026.

Saunders, R.C., Aggleton, J.P., 2007. Origin and topography of fibers contributing to the fornix in macaque monkeys. Hippocampus 17 (5), 396–411. https://doi.org/10.1002/hipo.20276.

Schilling, K.G., Petit, L., Rheault, F., Remedios, S., Pierpaoli, C., Anderson, A.W., et al., 2020. Brain connections derived from diffusion MRI tractography can be highly anatomically accurate—if we know where white matter pathways start, where they end, and where they do not go. Brain Struct. Funct. 225, 2387–2402. https://doi.org/10.1007/s00429-020-02129-z.

Shapiro, M.L., Riceberg, J.S., Seip-Cammack, K., Guise, K.G., 2014. Functional interactions of prefrontal cortex and the hippocampus in learning and memory. In: Space, Time and Memory in the Hippocampal Formation. Springer Vienna, Vienna, pp. 517–560.

Siapas, A.G., Lubenov, E.V., Wilson, M.A., 2005. Prefrontal phase locking to hippocampal theta oscillations. Neuron 46 (1), 141–151. https://doi.org/10.1016/j.neuron.2005.02.028.

Spellman, T., Rigotti, M., Ahmari, S., et al., 2015. Hippocampal–prefrontal input supports spatial encoding in working memory. Nature 522, 309–314. https://doi.org/10.1038/nature14445.

Starrett, M.J., Ekstrom, A.D., 2018. Perspective: assessing the flexible acquisition, integration, and deployment of human spatial representations and information. Front. Hum. Neurosci. 12, 281. https://doi.org/10.3389/fnhum.2018.00281.

Strange, B.A., Witter, M.P., Lein, E.S., Moser, E.I., 2014. Functional organization of the hippocampal longitudinal axis. Nat. Rev. Neurosci. 15 (10), 655–669. https://doi.org/10.1038/nrn3785.

Sutherland, R.J., Kolb, B., Whishaw, I.Q., 1982. Spatial mapping: definitive disruption by hippocampal or medial frontal cortical damage in the rat. Neurosci. Lett. 31 (3), 271–276. https://doi.org/10.1016/0304-3940(82)90032-5.

Swanson, L.W., Cowan, W.M., 1977. An autoradiographic study of the organization of the efferent connections of the hippocampal formation in the rat. J. Comp. Neurol. 172 (1), 49–84. https://doi.org/10.1002/cne.901720104.

Thomas, G.J., 1978. Delayed alternation in rats after pre-or postcommissural fornicotomy. J. Comp. Physiol. Psychol. 92 (6), 1128. https://doi.org/10.1037/h0077522.

Thornberry, C., Cimadevilla, J.M., Commins, S., 2021. Virtual morris water maze: opportunities and challenges. Rev. Neurosci. 32 (8), 887–903. https://doi.org/10.1515/revneuro-2020-0149.

Tomas Pereira, I., Burwell, R.D., 2015. Using the spatial learning index to evaluate performance on the water maze. Behav. Neurosci. 129 (4), 533–539. https://doi.org/10.1037/bne0000078.

Tonkiss, J., Feldon, J., Rawlins, J.N.P., 1990. Section of the descending columns of the fornix produces delay-and interference-dependent working memory deficits. Behav. Brain Res. 36 (1–2), 113–126. https://doi.org/10.1016/0166-4328(90)90166-C.

Tsivilis, D., Vann, S.D., Denby, C., Roberts, N., Mayes, A.R., Montaldi, D., Aggleton, J.P., 2008. A disproportionate role for the fornix and mammillary bodies in recall versus recognition memory. Nat. Neurosci. 11 (7), 834–842. https://doi.org/10.1038/nn.2149.

Van de Maele, T., Dhoedt, B., Verbelen, T., Pezzulo, G., 2024. A hierarchical active inference model of spatial alternation tasks and the hippocampal-prefrontal circuit. Nat. Commun. 15 (1), 9892. https://doi.org/10.1038/s41467-024-54257-3.

Vann, S.D., 2013. Dismantling the Papez circuit for memory in rats. eLife 2, e00736. https://doi.org/10.7554/eLife.00736.

Vann, S.D., Erichsen, J.T., O'Mara, S.M., Aggleton, J.P., 2011. Selective disconnection of the hippocampal formation projections to the mammillary bodies produces only mild deficits on spatial memory tasks: implications for fornix function. Hippocampus 21 (9), 945–957. https://doi.org/10.1002/hipo.20796.

Wagenmakers, E.J., Verhagen, J., Ly, A., Bakker, M., Lee, M.D., Matzke, D., et al., 2015. A power fallacy. Behav. Res. Methods 47, 913–917. https://doi.org/10.3758/s13428-014-0517-4.

Wagenmakers, E.J., Verhagen, J., Ly, A., 2016. How to quantify the evidence for the absence of a correlation. Behav. Res. Methods 48 (2), 413–426. https://doi.org/10.3758/s13428-015-0593-0.

Wang, G.W., Cai, J.X., 2008. Reversible disconnection of the hippocampal-prelimbic cortical circuit impairs spatial learning but not passive avoidance learning in rats. Neurobiol. Learn. Mem. 90 (2), 365–373. https://doi.org/10.1016/j.nlm.2008.05.009.

Warburton, E.C., Baird, A.L., Morgan, A., Muir, J.L., Aggleton, J.P., 2000. Disconnecting hippocampal projections to the anterior thalamus produces deficits on tests of spatial memory in rats. Eur. J. Neurosci. 12 (5), 1714–1726. https://doi.org/10.1046/j.1460-9568.2000.00039.x.

Weisberg, S.M., Ekstrom, A.D., 2021. Hippocampal volume and navigational ability: the map (ping) is not to scale. Neurosci. Biobehav. Rev. 126, 102–112. https://doi.org/10.1016/j.neubiorev.2021.03.012.

Woolley, D.G., Vermaercke, B., de Beeck, H.O., Wagemans, J., Gantois, I., D'Hooge, R., et al., 2010. Sex differences in human virtual water maze performance: novel measures reveal the relative contribution of directional responding and spatial knowledge. Behav. Brain Res. 208 (2), 408–414. https://doi.org/10.1016/j.bbr.2009.12.019.

Zhang, J., Yao, M., Jiang, T., Li, A., Gong, H., He, M., et al., 2025. A dorsal subiculum-medial mammillary body pathway for spatial memory. Mol. Psychiatr. 30, 5045–5057. https://doi.org/10.1038/s41380-025-03087-w.

Zhong, J.Y., Magnusson, K.R., Swarts, M.E., Clendinen, C.A., Reynolds, N.C., Moffat, S.D., 2017. The application of a rodent-based Morris water maze (MWM) protocol to an investigation of age-related differences in human spatial learning. Behav. Neurosci. 131 (6), 470. https://doi.org/10.1037/bne0000219.